Green Chemistry

Tuning the Selectivity of Electrochemical Levulinic Acid Reduction to 4-Hydroxyvaleric Acid: A Monomer for Biocompatible and Biodegradable Plastics

Journal:	*Green Chemistry*
Manuscript ID	GC-ART-08-2021-002826.R1
Article Type:	Paper
Date Submitted by the Author:	18-Oct-2021
Complete List of Authors:	Lucas, Francisco; University of Colorado Boulder, Chem. & Bio. Eng Fishler, Yuval; University of Colorado Boulder, Chem. & Bio. Eng. Holewinski, Adam; University of Colorado Boulder, Chem. & Bio. Eng.

Tuning the Selectivity of Electrochemical Levulinic Acid Reduction to 4-Hydroxyvaleric Acid: A Monomer for Biocompatible and Biodegradable Plastics

Francisco W. S. Lucas[1,2]*, Yuval Fishler[1,2], Adam Holewinski[1,2]*

[1]Department of Chemical and Biological Engineering, University of Colorado, Boulder, CO 80303, United States; [2]Renewable and Sustainable Energy Institute, University of Colorado, Boulder, CO 80303, United States.

*Corresponding authors: adam.holewinski@colorado.edu (A.H.), and willlucas@yahoo.com.br (F.W.S.L)

Abstract

Levulinic acid (LA) is a biomass-derived feedstock that can be converted to a wide array of value-added products; several of these can be accessed efficiently by electrochemical conversion. Herein, we present a study of factors governing LA conversion in electrochemical environments. Most notably, we identify an unprecedented pathway forming 4-hydroxyvaleric acid (HVA), a valuable monomer that can be used for production of bio-polyesters—specifically, poly(hydroxy acids)—as well as γ-valerolactone (GVL) (a green fuel/solvent) and other fine chemicals. This method shows >99.9% selectivity and >80% faradaic efficiency for conversion above 80%. Production rates higher than 40 g L^{-1} h^{-1} (or 200 kg L^{-1} $m^{-2}_{geom.}$ h^{-1}) were achieved; these are substantially higher than reports for compatible biochemical methods. We further identify mechanistic insights regarding the steering of selectivity toward this new pathway in comparison to known electrochemical routes toward valeric acid (VA) or to GVL. Finally, we provide a fast, sequential one-pot synthesis route to transform electrochemically-produced HVA to GVL with higher

overall selectivity and faradaic efficiency than can be achieved by direct aqueous electrochemical conversion of LA to GVL (96% conversion and >99.9% selectivity, giving a total yield of 93% from LA).

Keywords: Biomass, 4-hydroxypentanoic acid, valeric acid, γ-valerolactone, electrosynthesis, biopolymer.

1. Introduction

Levulinic acid (4-oxopentanoic acid, LA) has been identified as a highly versatile biomass-derived platform molecule, as highlighted by the U.S. Department of Energy[1] and a number of reports on biorefining for a sustainable chemical supply chain.[2–4] LA is produced at industrial-scale *via* acid-catalyzed hydrolysis of lignocellulose[2–4] and can be upgraded to several commodities and fine chemicals that are platforms for production of fuels and fuel-additives (e.g. 2-methyl-tetrahydrofuran, 5-nonanone, alkyl levulinates, γ-valerolactone), polymers (e.g. hydroxyvaleric acid, diphenolic acid), herbicides and pesticides (e.g. α-aminolevulinic acid), pharmaceuticals and food additives (e.g. alkyl levulinates, hydroxyvaleric acid, γ-valerolactone), and other materials and products.5 LA upgrading toward an assortment of these products has been demonstrated by thermo-, bio-, and electro-chemical routes.[5–8] Advantages of electrochemical valorization (both oxidative and reductive) over thermochemical methods can often include operability at near-ambient conditions and compatibility with aqueous feedstocks. In comparison to biochemical/enzymatic routes, electrochemistry generally offers much faster conversion rates and simple separations.[9–11] It is also

worth mentioning that electrochemical methods are in many cases scalable and have been used for the production of a variety of compounds in several chemical industries.[12,13]

Scheme 1 shows the major electrochemical transformations presently known to be accessible from LA; electro-oxidation and electro-reduction routes are organized, respectively, at the left (red arrows) and right (blue arrows) sides of the Scheme, with exemplary references for each also noted. It has been previously demonstrated that, through engineering of reaction conditions, LA can be reduced predominantly into valeric acid (VA) or γ-valerolactone (GVL); conversely, it can be oxidized into 4-hydroxybutanone, 3-butenone, or 2,7-octanedione. Octane can also be accessed in a second step *via* Kolbe oxidation of valeric acid or electro-hydrodeoxygenation of 2,7-octanedione.[13] The present work now adds 4-hydroxyvaleric acid (HVA, also known as 4-hydroxypropanoic acid, valued as a green monomer) to the list of tunable reduction products. We show >99.9% selectivity and >80% faradaic efficiency (FE) for >80% conversion and further provide a one-pot synthesis route to transform the HVA to GVL (96% conversion and >99.9% selectivity, giving a yield of 96% from LA). This route avoids nonaqueous mediated conditions previously required to generate GVL efficiently by electrosynthesis.[8]

Focusing on the reductive paths, selectivity between VA and GVL has been observed to depend on the pH of the supporting electrolyte. Strongly acidic media (0.5 – 1.0 M H_2SO_4) tend to favor the formation of VA,[14,15] while GVL has been mainly observed in neutral or alkaline conditions (pH 7.5 phosphate buffer[14] or 0.1 M NaOH[15]). For the acidic electrolyses, several works have shown high selectivities for

VA (> 85% amongst organic products) with high faradaic efficiencies (44 – 65%, for conversion > 70%).[13–17] At elevated pH, the highest FE for LA reduction to GVL in aqueous solutions was demonstrated by Schröder *at al.*[15] (20% FE, with 70% GVL selectivity) on an Fe cathode, while higher selectivity (amongst the organic products) was found by Li *et al.*[14] using a PbS cathode, albeit with lower FE (6.2%, with GVL selectivity 100%). Recently, Han *et al.*[8] also showed complete selectivity to GVL at much higher FE (79%), though conversion values were not mentioned, and the reaction was performed in an organic solvent with ionic liquid as supporting electrolyte (1-butyl-3-methylimidazolium tetrafluoroborate in acetonitrile). Concerning the cathode material, carbon, Al, Ti, Fe, Ni, Cu, Zn, Ga, Ag, Cd, In, Sn, Sb, and Pb have been tested, but Pb (or Pb-based) cathodes consistently show the highest combined FE and conversion.[15,17] Until now, HVA has only been proposed—not shown—as an intermediate in the electrochemical reduction of LA to GVL, and it has not before been generated as a product.[8,14,16,17]

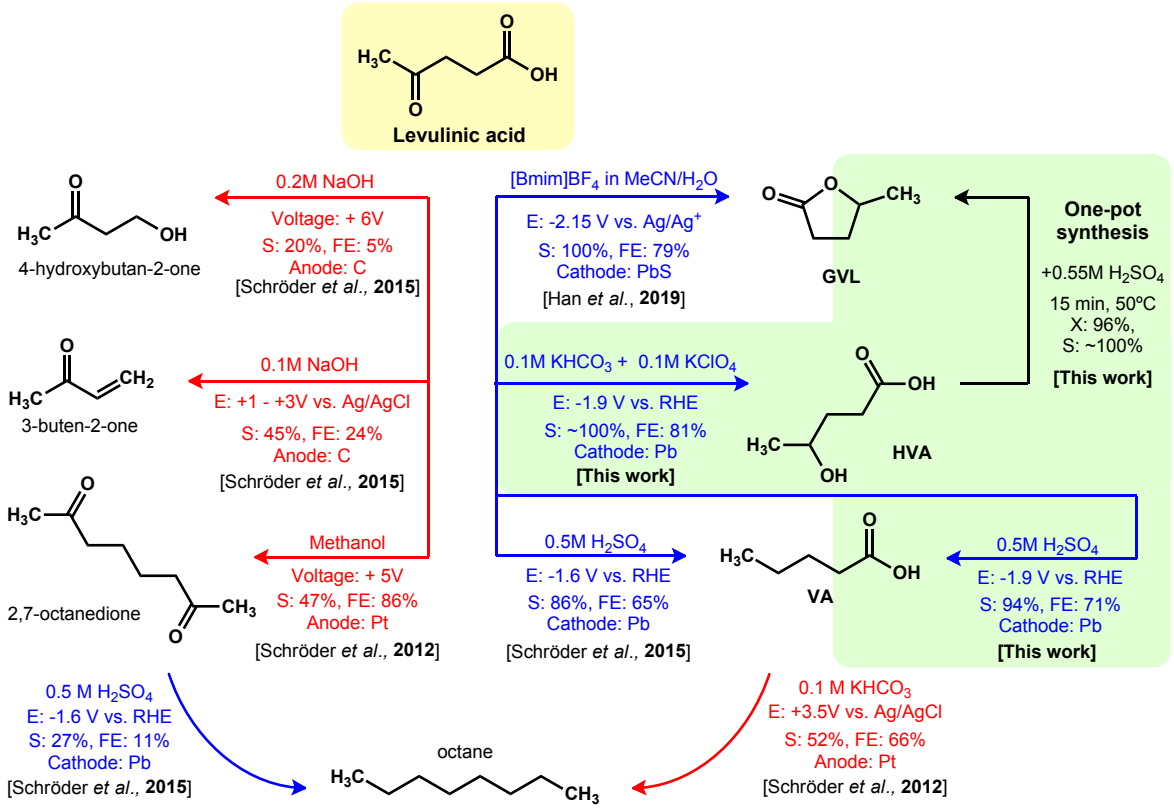

Scheme 1. *Electrochemical routes for levulinic acid upgrading. Data from Han et al.,*[8] *Schröder et al.,*[15,18] *and this work. Abbreviations are E: potential, FE: faradaic efficiency, S: selectivity, X: conversion.*

Selective routes to HVA are desirable as this hydroxycarboxylic acid is a versatile compound that can be used as a monomer for production of biodegradable and biocompatible polyesters—poly(hydroxy acids), PHAs—as well as other diverse commodities, fine chemicals, pesticides, and pharmaceuticals.[19,20] Focusing only on the biopolymers and bioplastics industry, the projected global market will reach USD ~28 billion by 2025 and HVA-derived polymers have the potential to fill a significant fraction of this demand with a variety of homopolymers and co-polymers that exhibit outstanding physico-chemical properties for biomedical use, packaging, and other technological applications.[21–25] Several companies including Metabolix, P&G, and

TEPHA already manufacture PHA products,26 but the application of these polymers is still limited due to absence of technology to produce the HVA monomer efficiently on a large scale. Polymerization routes are discussed elsewhere, but focusing on HVA monomer,[27] it has been previously produced *via* chemical depolymerization of intracellular PHAs (polyhydroxyalkanoates, which are synthesized by some types of bacteria)[27] and by direct biochemical reduction of LA.[19] The former method suffers from the use of harsh conditions, expensive catalysts, and toxic solvents. Low yields from incomplete depolymerization are also common—typically, only 30 – 50% of the carbon source fed to the bacteria is converted into PHAs, while the recovery of converted hydroxyacid monomers after hydrolysis has also not been reported above 88%. In contrast, the direct biochemical methods are generally performed under milder conditions (closer to neutral pH, aqueous solution, room-temperature). However, they still have shown relatively slow rates of production, hindering industrial-scale prospects for this method. Two of the most efficient biochemical demonstrations were by Sathesh-Prabu *at al*.20 and Kim *at al.*[28] Sathesh-Prabu *at al*. showed HVA production of 50 g L^{-1} from LA (with 97% conversion) in 100 h (*i.e.* 0.5 g L^{-1} h^{-1}), using a 250 mL bioreactor containing a genetically modified *Pseudomonas putida KT2440* strain culture.20 Kim *at al.*[28] developed a large-scale method for production of HVA *via* enzymatic reduction of LA using an engineered 3-hydroxybutyrate dehydrogenase (3HBDH) from an *Escherichia coli* strain. With this method, 4.2 g L^{-1} h^{-1} of HVA could be produced (titer 100 g L^{-1} in a 5-L bioreactor), with 92% LA conversion.[28]

Herein, we discuss a number of mechanistic insights regarding LA reduction (LAR) into VA, GVL and HVL, and we show a batch electrochemical method for

conversion of LA into HVA at a production rate higher than 40 g L^{-1} h^{-1} (i.e., 200 kg L^{-1} $m^{-2}_{geom.}$ h^{-1}) with >99.9 % selectivity, and conversion and faradaic efficiency both above 80% for one stoichiometric equivalent of charge ($2e^-$/LA) passed. This rate is more than nine times higher than the highest recorded biochemical methods,[19,20,27,28] and it is expected that this can be increased by further reaction engineering (optimizing mass transport, reactor area/volume (A/V) ratio, etc). Complete LA conversion could also be achieved, albeit with decreasing rate and FE toward the end of electrolysis. We also present an easy one-pot synthetic method to convert HVA into GVL that proceeds in 15 min with 100% selectivity and 96% conversion.

2. Experimental Methods

2.1. Materials and Chemicals

All chemicals were of analytical grade and were used directly without further purification: Levulinic acid (Sigma-Aldrich, >99.5%), Valeric acid (Sigma-Aldrich, >99.5%), γ-valerolactone (Sigma-Aldrich, >99.5%), Pb plate (Goodfellow, 99.99+%), $LiClO_4$ (Sigma-Aldrich, >99.9%), $NaClO_4$ (Sigma-Aldrich, >99.9%), $KClO_4$ (Sigma-Aldrich, >99.9%), $CsClO_4$ (Sigma-Aldrich, >99.9%), $LiHCO_3$ (Sigma-Aldrich, >99.5%), $NaHCO_3$ (Sigma-Aldrich, >99.5%), $KHCO_3$ (Sigma-Aldrich, >99.5%), $CsHCO_3$ (Sigma-Aldrich, >99.5%), NaH_2PO_4 (Synth, >95%), Na_2HPO_4 (Synth, >95%), Suprapure H_2SO_4 (Sigma-Aldrich, >99.999%), Suprapure $HClO_4$ (Sigma-Aldrich, >99.999%), Acetic acid (Sigma-Aldrich, >99.5%), Potassium acetate (Sigma-Aldrich, >99.5%), 0.05 wt.% sodium 3-(trimethylsilyl)-2,2,3,3-tetradeuteropropionate (TMSP) in D_2O (99.9 at. % D, Sigma-Aldrich), Argon (UHP,

Airgas Inc.). Solutions were prepared using ultra-pure deionized water with a specific resistance of >18.2 MΩ cm (purified by a Milli-Q, Milipore Inc.).

2.2. Electrochemical experiments

Electrochemical experiments were carried out using a conventional three-electrode H-type cell, with cathodic and anodic compartments (10 mL each) separated by a proton- or anion-exchange membrane (Nafion® 117 or Fumapem® FAA-3-50, Fuel Cell Store), depending on pH. A 3 cm^2 Pt-plate and a leak-free $Ag/AgCl/Cl^-_{(sat.\ KCl)}$ were used as auxiliary and reference electrodes (AE, RE), respectively. The RE was calibrated against a reversible hydrogen electrode (RHE), and all potentials in this work are referenced to RHE. A 2 cm^2 Pb (C-shaped) plate was used as the working electrode (WE). The WE was cleaned in 30 % v/v HNO_3 and rinsed in deionized water immediately before each experiment. The electrochemical cell was degassed with $Ar_{(g)}$ and the temperature was controlled by a thermostatic bath (Fisher Scientific). Electrochemical measurements were performed with a potentiostat/galvanostat (Gamry Instruments, Reference 3000). Uncompensated resistance (R_u) was measured by electrochemical impedance spectroscopy (EIS) and/or current interrupt mode, and all electrochemical measurements were R_u corrected. Electrolysis experiments were performed by chronocoulometry, controlling the exact equivalent charge for each experiment (2F or 4F per LA mol) and under constant magnetic stirring (1500 rpm, if not specified).

2.3. Product identification and quantification

Products of electrolysis were identified and quantified by ^{1}H NMR and liquid chromatography (LC); procedure details are organized in the Supporting Information. For NMR analysis, a Bruker AVANCE-III 400 MHz NMR spectrometer was used, and LC analyses were performed in an Advion 2000 HPLC equipped with a 300 mm x 6.5 mm sulfonated polystyrene gel column (Hi-Plex H, Agilent), a UV diode array detector (DAD), and an Advion Expression Compact Mass Spectrometer (S Series). The experiments for optimization of mobile phase, elution rate, and column temperature, as well as the external calibration curves for levulinic acid (LA), valeric acid (VA), γ-valerolactone (GVL), and 4-hydroxyvaleric acid (HVA) are described in the Supporting Information. The chemical and analytical distinction between GVL and HVA was based on the chemical shift signature and molecular ion fragment of their ^{1}H NMR and mass spectra, respectively.

2.4. *in-situ* ATR-FTIR

A Nicolet 6700 FTIR spectrometer (Thermo Fisher Scientific) with VeeMAX^{TM} III (PIKE Technologies) ATR configuration chamber was used for *in-situ* ATR-FTIR experiments. The spectroelectrochemical experiments were performed in a J1W Jackfish cell (PIKE Technologies) with a PTFE/PEEK base, and IRUBIS Si(100) specialized 1-ATR element (single-bounce ATR crystal). A polycrystalline Au electrode was chemically deposited (electroless deposition) based on a procedure first established and demonstrated by Osawa et al.[29] The experiment consisted of two stages: electrodeposition of Pb onto the polycrystalline Au electrode, followed by demonstration of Pb-H_2 formation with electrochemical ATR-FTIR. The Pb film was electrodeposited from a 1 mM $Pb(ClO_4)_2$ solution, at -0.4V vs $Ag/AgCl_{sat.\ KCl}$ for

70 mC cm^{-2}. The spectroelectrochemical experiment was then done as a differential potential step scan in 0.1 M $KClO_4$ electrolyte. The FTIR background (64 interferograms) was taken at 0.1 V vs RHE, and spectra were taken at different sequential potential steps from -0.05 to -1.90 V vs RHE, with incremental steps of -150 mV. To allow stable behavior resulting in a quasi steady-state (at each potential during the potential step scan), spectrum collection was begun 10 seconds after each new bias application. For each potential measurement, the electrode was kept polarized under the potential applied in the prior measurement (without relaxation) to exclude double layer charging/discharging effects. Each measurement in the series consists of 128 interferograms averaged by the instrument software (OMNIC™ Specta Software).

3. Results and discussion

3.1. Effect of pH on selectivity and mechanistic implications

Product distributions and rates of levulinic acid reduction (LAR) were first evaluated under a range of controlled pH conditions in order to assess their impact and to gain some mechanistic insight. These initial electrolyses were performed at a constant temperature of 20°C, with an initial LA concentration of 0.1 mol L^{-1} and a total charge of 4F per mol of LA passed (~1.5 – 2.0h of electrolysis). Pb was used as the working electrode, and a potential of -1.9 V vs. RHE was chosen, as exploratory studies revealed this condition to balance high rate and faradaic efficiency against the propensity of Pb toward cathodic corrosion (disintegration) at more extreme negative potentials—similar observations have been made in other

studies of LAR using Pb.[13–17] For intermediate pH solutions, 0.1 M $KClO_4$ (a neutral salt) was added to buffer solutions as a co-supporting electrolyte to maintain sufficient conductivity without impacting the pH. At the end of each electrolysis, the final pH of the solutions was also measured, and it was observed that all strongly acidic/basic and buffered conditions were stable.

Figure 1 shows faradaic efficiencies for the different LAR products, along with LA conversions, for electrolyses performed across various pH conditions. Corresponding selectivities (S%, organic conversion basis) can be seen in Figure S4, and additional electrolysis conditions with other supporting electrolytes can be seen in Table S1 (Entries 1 – 10). Mass balances for all electrolyses were above 95%, meaning that LA and its reduction products do not easily cross the ion-exchange membranes and all major products were identifiable. For bicarbonate- and carbonate-containing electrolytes, a small portion of the current (< 3%) was lost through the formation of formic acid (FA) from electrochemical reduction of CO_2. This comes from a slow equilibrium conversion of carbonate species to CO_2—cells were always thoroughly purged before electrolysis.[29]

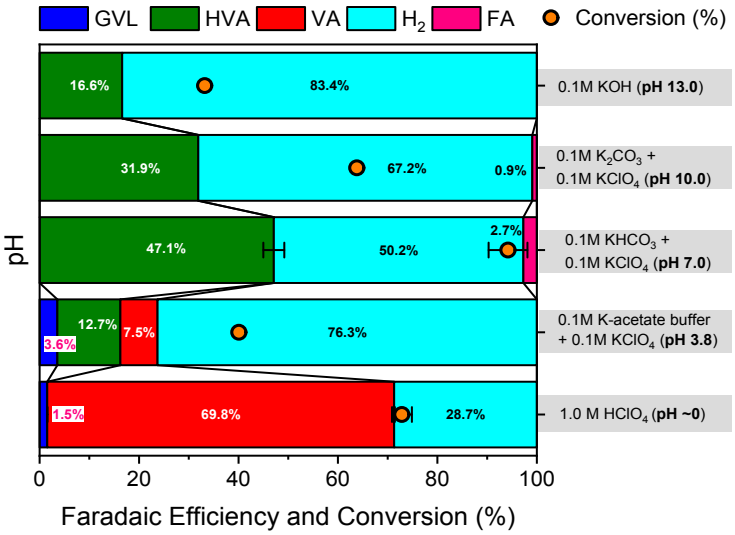

Figure 1. *pH effects for electrolyses performed with 0.1 mol L^{-1} LA, at -1.9 V vs. RHE, with passage of 4 F/mol LA. Conversion and faradaic efficiencies are shown for each product (VA: valeric acid, HVA: 4-hydroxyvaleric acid, GVL: γ-valerolactone, and FA: formic acid).*

In 1.0 M $HClO_4$ (pH ~0), the FE toward VA was nearly 70%, with trace GVL production and overall conversion above 80%. For comparison, similar electrolyses with 0.5 M H_2SO_4 (pure, and with a perchlorate containing co-supporting electrolyte: 0.5 M H_2SO_4 + 0.1 M $KClO_4$) showed virtually identical results (Figure S5 and Table S1, Entries 1-3). This suggests that the anions have a low impact on the mechanism for the formation of VA and GVL and that alkali cations do not strongly compete with H^+ and LA for Pb surface sites (at this pH). When the pH was increased to 3.8, the total faradaic efficiency for LAR decreased, and the selectivity shifted dramatically to just 18.7% VA, with 17.9% GVL production and 63.4% HVA appearing (^{1}H NMR

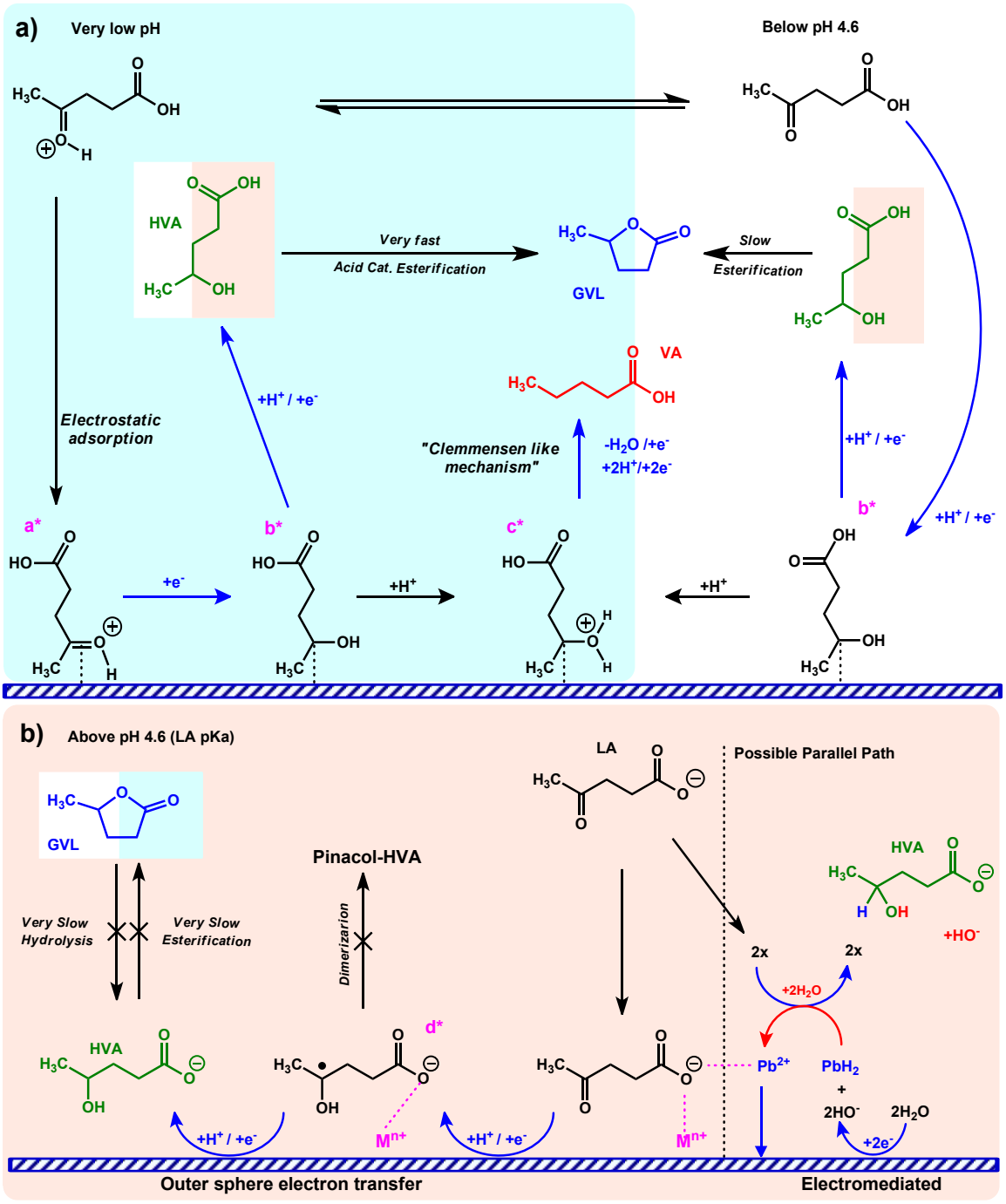

Scheme 2. *Levulinic acid (LA) reduction reaction: proposed routes for the formation of valeric acid (VA), 4-hydroxyvaleric acid (HVA), and γ-valerolactone (GVL). Mechanisms are shown for pH below (a) and above (b) the LA pKa ~4.6. Very low pH and weakly acidic pH are shown with blue and white backgrounds, respectively, while pH above the pKa has a red background.* M^{n+}*= electrostatically adsorbed cation.*

spectrum shown in Figure S6). At pH 7 and above, VA and GVL were not detected, and, using MS and ^{1}H-NMR, it was possible to prove that each neutral-to-alkaline condition produces HVA with >99.9% selectivity (Figure S7). These results also exclude the presence of HVA dimer (Pinacol-HVA).

Since HVA has not previously been observed in this reaction, it is prudent to consider the likely mechanistic pathways governing LA reduction selectivity. Based on the observed pH trends, we propose that the formation of VA and GVL occurs through a surface-mediated mechanism, while HVA is formed mainly *via* an outer sphere electron transfer (OSET) route, favored at higher pH (above the pKa of LA), as presented in Scheme 2. An electromediated mechanism involving solution phase Pb-species is also possible (discussed further below). The first discriminating factor to be considered is that, near pH 0, a portion of LA molecules will be protonated at the ketonic-carbonyl oxygen. Neutral LA (and/or its enol form) may also react, but evidence has been presented by several authors[10,30] that the cationic form of aliphatic ketones (here LA-H^{+}) promotes electrostatic adsorption on the cathode surface (intermediate **a***) under the influence of the electric field below the potential of zero charge (PZC). The local concentration of protons at the surface may also be enriched and drive equilibrium toward LA-H^{+}, though this depends on the rate of reaction and presence of other cations (here K^{+} addition did not impact the rate, as noted above). Even if the population of LA-H^{+} is very low, the mechanism can in principle proceed due to rapid acid-base equilibrium being maintained as this protonated form is consumed. The rate of adsorption of these species effectively balances with the adsorption of protons and allows good competition against the

parallel hydrogen evolution reaction (HER), making the total FE for reduction of LA the highest across all pH conditions.

Thus, it is expected that intermediate **a*** is electrochemically reduced to chemically adsorbed intermediate **b*** (bound by the former carbonyl carbon), which can further be reduced to HVA or protonated at the alcohol group to form intermediate **c***. The alcohol protonation will be much more favorable than carbonyl protonation, and thus regardless of whether LA-H^+ or neutral LA initially react, the predominant pathway in strong acid is apparently through intermediate **c***, as it should terminate with hydrodeoxygenation to form VA under a well-known Clemmensen reduction mechanism (several steps are not shown in the scheme).[31] Any HVA that forms (from **b***) should be immediately converted to GVL *via* acid-catalyzed, homogeneous, intramolecular esterification (lactonization), explaining why HVA is not detected in strong acid but appears alongside GVL at pH 3.8. Under the milder acidic conditions, cationic LA-H^+ species will cease to be present, but the neutral LA molecule can still adsorb and form intermediate **b*** (by $1e^-$ reduction). Since VA formation should still require acid-catalyzed hydrodeoxygenation of intermediate **c***, this pathway is diminished at less acidic pH. Combined with slower homogeneous conversion of HVA into GVL, all three products are detected in weak acid with HVA predominating.

Shifting to the pH window from 7 to 13 (above the pKa of LA, 4.6), it is not expected that levulinate ions (LA^-) can adsorb on the electrode since it bears a strong negative charge—the operating potential of -1.9 V vs. RHE at pH 7 is > 1.6 V more negative than the PZC for lead electrodes (about -0.7 V vs. SHE)[32], and even more so at higher pH. Since reduction does in fact proceed, it can be expected that

either neutral LA—continually restored near the surface by acid-base equilibrium—adsorbs, or alternatively, the charge screening by alkali cations present in the Helmholtz layer is sufficient to permit LA^- a close enough approach to the surface to be reduced *via* OSET. We suggest predominance of solution phase reduction for two reasons: (i) unlike the case of LA-H^+, the minority neutral molecule is not actively driven to the surface by the electric field, and (ii) no dimeric species are formed. Reduction and protonation of LA^- would yield a 4-hydroxycarboxylic radical (intermediate **d***), which can be further reduced and protonated to HVA. It is common in the electrochemical reduction of ketones and aldehydes for radicals such as intermediate **d*** to dimerize in neutral or alkaline environments, forming a pinacol product (vicinal diol);[10] however, the anionic and solvated nature of intermediate **d*** can create repulsion, whereas neutral adsorbed intermediates would be expected to show some dimer yield. We thus attribute the reactivity to solution-phase LA^-. Extra non-electrochemical control experiments (cf. Supporting Information, "Homogeneous hydrolysis of GVL", Figure S11) were also used to verify that GVL cannot be hydrolyzed to HVA under the experimental conditions used for these electrolyses, confirming that HVA is formed directly and terminally.

Interestingly, increasing the pH in the neutral-to-alkaline regime caused a continual decrease in FE_{HVA}, favoring the HER *via* H_2O reduction. In principle, several effects could play a role, and their relative importance likely varies with increasing pH. It should first be noted that even with the highest practical stirring rates, the reaction operated in a regime with significant influence from mass transfer with respect to LA under most experimental conditions (see Figure S8 for characterization with variable stirring rates and discussion of mass transfer). This

was always the case for pH conditions that were selective to HVA, and thus we emphasize that the reported data should be interpreted in this context. The rate of HER is well known to increase moving from neutral to alkaline pHs for a given potential vs. RHE (overpotential thus increasing on an SHE scale) and to remain controlled by kinetics due to water acting as the proton source in these conditions.[33,34] This reaction becomes increasingly predominant as pH rises, while we find the partial current to LAR stays roughly constant moving from pH 7 to 10 (consistent with reaching mass transfer limitation), lowering the FE. However, the total current and LAR current both decrease at pH 13 (c.f. Table S1), and it is critical to recall that under these extremely cathodic conditions, Pb electrodes can undergo several additional side reactions.

First, alkali cations can be electrodeposited onto/into Pb surface, forming Pb-alkali amalgams (Eq. 1). This is a century-old phenomenon known as implantation[35–37] and is also observed for electrodes such as In, Ga, Hg, and Sn, among others.[38] Second, Pb electrodes can form hydrides at these very negative potentials (Eq. 2).[36] Both phenomena (alkali implantation and hydride formation) further cause electrode lixiviation or disintegration[35–37], schematized in Eqs. 3, 4, and 5. These processes consume 1F per mol of Pb-alkali amalgam or 2F per mol of PbH_2 and generate an equivalent amount of H_2 (still accounted in total FE); this can contribute to decreases in FE_{LAR} as pH rises, although a drop in total current at high pH suggests that all pathways are altered and the parasitic pathways are not simply additive with the main faradaic reactions. We found that disintegration was accelerated with visible colloidal Pb forming when the concentration of alkalis was increased at pH 13 by adding 0.1 mol L^{-1} $KClO_4$ to the 0.1 M KOH electrolyte (cf. Entry 10 – Table S1). This

supports the suggestion that the FE becomes significantly influenced by parasitic pathways mediated by Pb-electrolyte interactions at high pH.

$$M^{+}_{(aq)} + Pb_{(s)} + 1e^{-} \rightarrow (M)Pb_{(s)} \quad \text{(eq. 1)}$$

$$Pb_{(s)} + 2H_2O_{(l)} + 2e^{-} \rightarrow PbH_{2(aq)} + 2OH^{-}_{(aq)} \quad \text{(eq. 2)}$$

$$2(M)Pb_{(s)} + 2H_2O \rightarrow 2Pb_{(s,\ colloidal)} + 2M^{+}_{(aq)} + 2OH^{-}_{(aq)} + \mathbf{H_{2(g)}} \quad \text{(eq. 3)}$$

$$PbH_{2(aq)} \rightarrow Pb_{(s,\ colloidal)} + \mathbf{H_{2(g)}} \quad \text{(eq. 4)}$$

$$PbH_{2(aq)} + 2H_2O_{(l)} \rightarrow Pb(OH)_{2(s,\ colloidal)} + \mathbf{H_{2(g)}} \quad \text{(eq. 5)}$$

Aside from mediation of HER, it is possible that PbH_2 molecules would also mediate the reduction of LA (as shown in Scheme 2). After formation of Pb(II) hydride from Pb^0 ($2e^-$ per mol, Eq. 2), each hydride moiety (H^-) would promote the reduction of LA to HVA (forming 2 HVA molecules by transfer of $2e^-$ *each*). The resulting Pb^{2+} ions would then be electrodeposited back as Pb^0, closing the electromediation cycle. The formation of two HVA molecules would involve a total transfer of $4e^-$ and remain accounted in the FE. To understand the possible interplay with such effects at more practically-relevant conditions, we next discuss the potential dependence at neutral pH in the following Section.

3.2. Potential effects

Focusing on the most ideal pH condition for HVA formation (pH 7), the effects of potential were evaluated to further understand and optimize the factors governing faradaic efficiency (Figure 2a). Cyclic voltammetry studies in 0.1 M $KHCO_3$ + 0.1 M $KClO_4$ with and without 100 mM LA (shown in Supporting Information, Figure S9)

showed that LA reduction becomes significant at potentials more negative than c.a. -0.9 V vs. RHE. The presence of LA also appeared to have a partial inhibitory effect on disintegration, as continued cycling to -1.9 V was stable in LA, but without LA led to formation of a white colloid (possibly lead hydroxide, Eq. 5), which eventually became dark-gray (lead hydroxide conversion to PbO_2 or colloidal Pb formed from PbH_2). When extending to more negative potentials (lower than -1.9 V) the disintegration products were observed regardless of the presence of LA. Thus, operating potentials from -1.1 V to a limit of -1.9 V vs. RHE were focused on to evaluate the influence on FE_{HVA} and rate of HVA production (i_{HVA}). This is shown in Figure 2a (now, using $2F/mol_{LA}$ since HVA is the only major product).

It was observed that FE_{HVA} and i_{HVA} both linearly increased toward more negative potentials, though with an almost constant total average current (total including HER) from -1.3 V out to -1.9 V (cf. Table S1). A similar trend was also observed at 50 ºC (Figure S10). Given that the transition toward mass transfer limitation of LAR is already observable at small overpotentials and lower temperature conditions (Figure S8), this collective behavior suggests some additional effects that are not captured in a typical reaction-diffusion framework with Butler-Volmer type kinetics. We suggest there to be a mixture of effects, possibly related to implantation and hydride formation reactions changing the surface and electronic structure of the electrode and/or leading to increase of the electro-mediated path in parallel. Changes to double layer structure and solvent dynamics influencing HER are also possible, though these are less likely to influence the LAR if it is already fully transport-limited.

Concerning the possibility of an electromediated path for LAR, it is known that the standard thermodynamic potential for formation of PbH_2 (i.e. at unit activity) is -1.92 V vs. RHE in pH 7.[40] Per the Nernst equation, it could be expected that PbH_2 may begin forming under significantly less negative potentials. To assess the electrochemical formation of PbH_2 at the relevant conditions, *in situ* ATR-FTIR spectra were collected for a Pb thin film electrode sequentially polarized from -0.05 to -1.90 V vs. RHE in the absence of LA (Figure 2b). This experiment shows the formation of (detectable) lead hydride starting around -1.60 V vs. RHE, evidenced by the appearance of a peak at about 1620 cm^{-1} associated with a Pb-H stretch. Based on the abrupt growth in IR intensity, it might be inferred that if PbH_2 mediation were becoming the main route for reduction of LA, an abrupt increase in rate and FE would also be expected toward more negative potentials. On the other hand, mass transfer effects could obscure such behavior. We suggest that, since the formation of HVA is already observed at 0.5 V smaller overpotential than PbH_2 is observed (corresponding to orders of magnitude slower PbH_2 production), that the electromediation mechanism represents at most a parallel contribution to HVA formation, alongside the OSET path. Decomposition and/or hydrolysis of PbH_2 would likely be faster than mediated LA reduction (a second order process), and thus we would not expect continual improvement in the FE at larger overpotentials if this path accounted for the dominant portion of current. Conversely, a final possibility could be that the presence of Pb^{2+} formed in solution during mediation events could make complexes with LA^- (e.g. $[LA\text{-}Pb]^+$) and thus drive an additional LA toward the electrode for reduction by OSET.

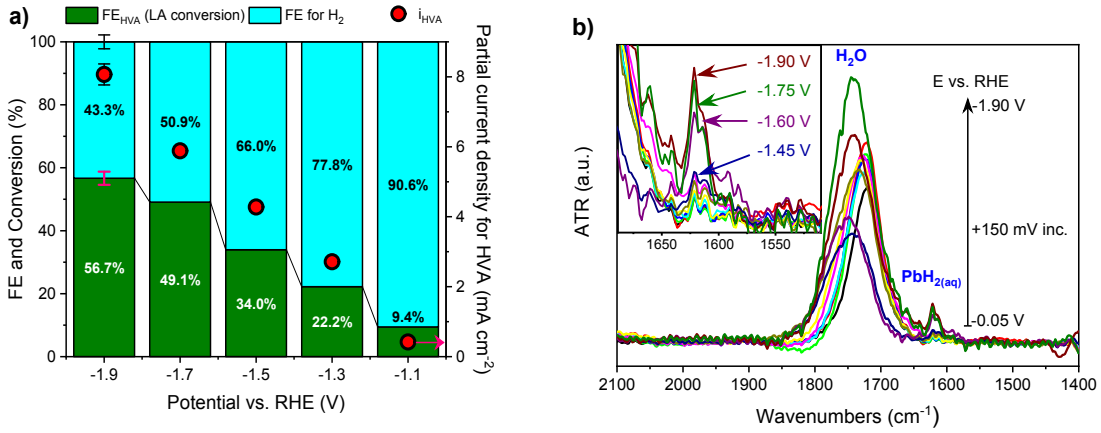

Figure 2. *a) Effect of potential for electrolyses carried out in 0.1 M $KHCO_3$ + 0.1 M $KClO_4$ at 20 ºC, and with total charge of 2 F/mol of LA. Since HVA is the only organic product, conversion for LA and faradaic efficiency for HVA are numerically equal. b) In-situ ATR-FTIR spectra for Pb film polarized at different potentials from -0.05 V to -1.90 V vs. RHE, with steps of 150 mV, in 0.1 M $KHCO_3$ + 0.1 M $KClO_4$ at 20 ºC.*

3.3. Impact of temperature, cation, and initial concentration

Several additional operating variables were investigated and found to have notable, though less decisive effects on the production of HVA (holding optimized pH and potential fixed). First, the impact of temperature was investigated. Upon increasing temperature from 20°C to 50ºC, it was observed that both reaction rates (LAR and HER) increased by roughly a factor of two (Figure 3), with the LAR increasing slightly more and raising the FE to HVA from 55% to 70%. Given an array of competing effects, the source of improved FE can presently only be speculated. The apparent activation barrier associated with HER kinetics is evidently lower than that associated with the mass transfer coefficient of LA. This could make sense in the context that the rate of water reduction far below electrode PZCs has been suggested to become governed by the dynamics of solvent reorganization rather

than the rate of electron transfer.[41] Other effects related to double layer structure or the local permittivity may also be involved but are beyond the scope of the present study.

Next, the influence of cations on LAR was evaluated. As can be seen in Figure 3, the rate of HVA formation increases in inverse proportion to the size of hydrated cation in the order $Cs^+ > K^+ > Na^+ >> Li^+$. The effect is small but is noteworthy as the FE_{HVA} does not follow the same trend—a slight maximum is instead found with Na^+ and K^+ cations. Recalling that virtually all LA molecules are deprotonated at this pH, screening effects or more specific interactions in the double layer may play a role (to the small extent that kinetics may still be relevant). It is known that Cs^+, having the smallest hydrated radius (and thus the highest surface density of cations), creates the most compact double layer potential profile, while Li^+ screens the electrode potential least effectively;[42,43] levulinate ions may thus be electrostatically stabilized closer to the electrode in the presence of Cs^+. Similar effects are also commonly observed and understood for OSET reactions between two anionic complexes.[43] At the same time, smaller hydrated cations are also generally associated with suppression of HER,[44] and thus the decrease observed in FE_{HVA} when moving toward Cs^+ suggests an additional competing effect. The leveling off of FE for K^+ and downward shift with Cs^+ is likely caused by their implantation in Pb, which we earlier established to decrease FE and which is known to be preferred with the trend $Cs^+ > K^+ \sim Na^+ > Li^+$.[35–37] Cs^+ implantation is particularly favorable due to the large difference in electronegativity between Cs and Pb, as well as their similar atomic radii.[45] Formation of PbH_2 and subsequent mediated mechanisms may also be promoted on heavily implanted electrodes.

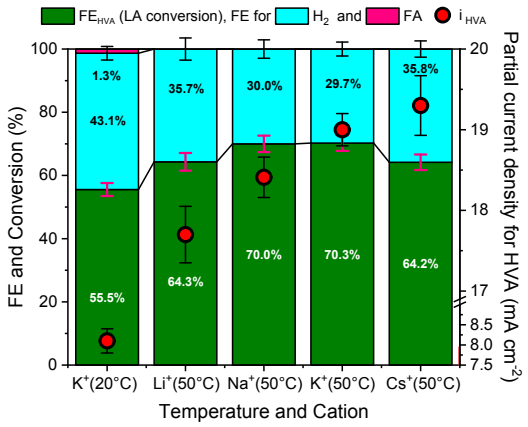

Figure 3. *Temperature and cation effects. Faradaic efficiencies, product distribution, LA conversion, and partial current density for HVA formation (i_{HVA}). Electrolysis performed in 0.1 M $MHCO_3$ + 0.1 M $MClO_4$ (pH 7, where M = Li^+, Na^+, K^+, and Cs^+), at 20 or 50 ºC, and with total charge of 2 F/mol of LA Since HVA is the only organic product, conversion for LA and faradaic efficiency for HVA are numerically equal.*

Finally, having roughly optimized the other operating conditions to produce HVA, the effects of the initial concentration of LA ($[LA]_{initial}$) were investigated to see if the rate of HVA production could be further improved. Electrolyses were carried out on 0.1, 0.2, and 0.4 M LA (close to the solubility limit of potassium levulinate) solutions at 50ºC. The production of HVA (quantified by HPLC) was followed after passing electric charges of 0.5, 1.0, 1.5, 2.0, 2.5, and 3.0 F / mol of LA. Just as a proof of concept, we also found the consumption of LA could be followed by simple *in-line* UV-vis spectrometry (cf. methodology in Supporting Information, Figure S12), since this reaction has ~100% selectivity toward HVA; this could be used as a simple method for *operando* characterization of HVA production, even at industrial scale. The time profiles of the electrolyses are shown in Figure 4, and as could be expected, FE_{HVA} increased as a function of $[LA]_{initial}$. It was also notable that even at high

conversion, the FE remained higher for equivalent concentrations of LA—in other words: comparing the more concentrated trials at higher conversion to the less concentrated trials at lower conversion, it can be concluded that higher HVA product concentration was also beneficial to the FE toward LAR. Speculatively, since coulombic effects likely prevent adsorption at this pH, the concentration effect may relate to a decrease (as conversion rises) in the transference number of the levulinate ion, for which migration and diffusion cause competing driving forces for transport to the electrode.

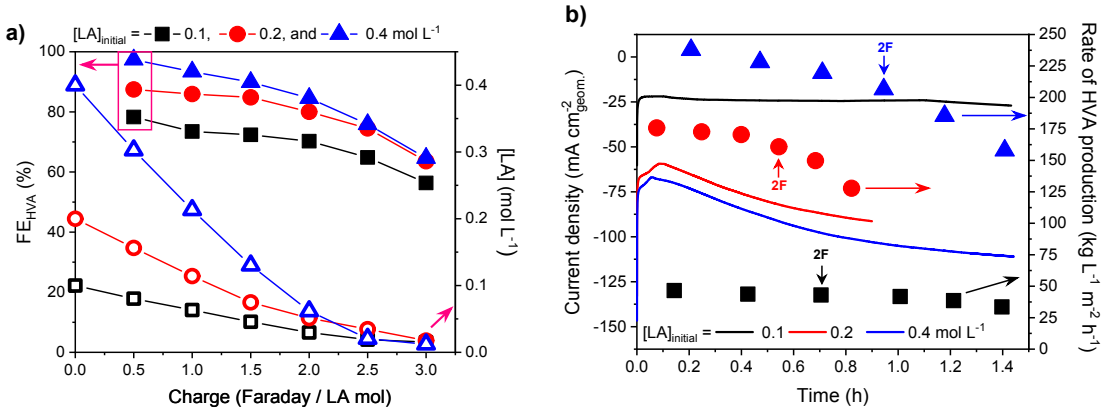

Figure 4. *Effect of initial concentration of LA ($[LA]_{initial}$).* ***a)*** *Faradaic efficiency and concentration of LA vs. charge passed for $[LA]_{initial}$ = 0.1 mol L^{-1}, 0.2 mol L^{-1}, and 0.4 mol L^{-1} during electrolyses carried out in 0.1 M $KHCO_3$ + 0.1 M $KClO_4$, at -1.9 V vs. RHE and 50 °C.* ***b)*** *Current density and rate of HVA production for same trials as a function of time (batch reaction rates based on the electrode geometric area and reactor size).*

Thus, amongst the evaluated conditions, it was possible to achieve HVA production rates from ~40 (for $[LA]_{initial}$ = 0.1 mol L^{-1}) to ~200 kg L^{-1} $m^{-2}_{geom.}$ H^{-1} (for $[LA]_{initial}$ = 0.4 mol L^{-1}) with conversion above 75% while maintaining an FE_{HVA} of 70 – 85% (stopping at 2F / mol of LA). Taking into account the reactor geometry (0.01

L divided-electrochemical reactor with electrode area/reactor volume (A/V) ratio of 0.02 m^2 L^{-1}), this maximum rate of 200 kg L^{-1} $m^{-2}_{geom.}$ h^{-1} (obtained with conversion and FE_{HVA} of 85% for $[LA]_{initial}$ = 0.4 mol L^{-1}) gives a titer of 40 g L^{-1} in one hour. This rate is more than nine times higher than that obtained for the most efficient reported biochemical methods[19,20,27,28] and could be further increased by optimizing the mass transport and reactor A/V ratio.

3.4. Conversion of HVA to GVL

Given the new route to make HVA efficiently, a one-pot electrochemical-chemical method of conversion of HVA into GVL is proposed as an alternative method of upgrading LA into GVL under aqueous conditions. Using the electrolysis carried out with $[LA]_{initial}$ = 0.4 mol L^{-1} and 3F / mol_{LA} (which gives 97% conversion, FE of 65%, and HVA production rate of ~32 g L^{-1} h^{-1}), we found a fast method of converting HVA into GVL by simply adding 30 µL of H_2SO_4 per mL of electrolyte (resulting in 0.55 M), as depicted in Scheme 3. As can be seen by ^{1}H-NMR (Figure S13), in 15 min, 96% of HVA was converted into GVL with >99.9% selectivity. The resulting 0.37 mol L^{-1} GVL solution contains only 4 mol % HVA and 3 mol % LA as impurities, illustrating this as a promising method of upgrading LA to GVL. Up to now, the most efficient aqueous electrochemical method for producing GVL from LA shows only 75% selectivity with FE_{GVL} and conversion of 20% and 25%, respectively.[15] While a full technoeconomic analysis is beyond the present scope, it may be noted that conventional thermochemical methods of LA hydrogenation to GVL generally involve high temperature and hydrogen pressure (70 – 270 ºC, and

0.5 – 150 MPa, respectively) and different precious metal-based catalysts (commonly Ru or Pt-based materials).[46–48]

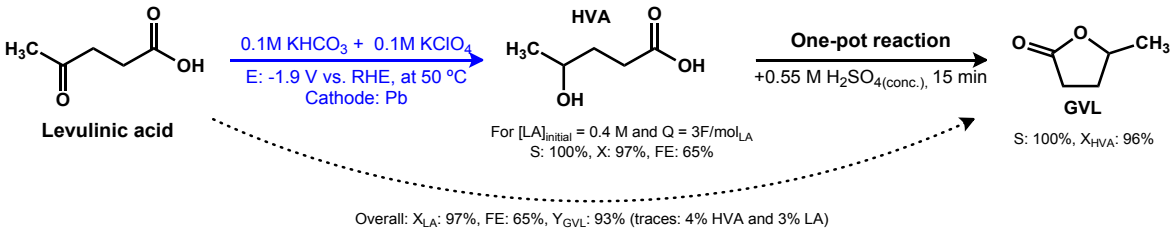

Scheme 3. *One-pot electrochemical-chemical method of upgrading LA into GVL.*

Conclusion

The impacts of pH, potential, temperature, cations, and concentration of reactant were studied to understand their influence on the selectivity and efficiency of electrochemical levulinic acid reduction (LAR). At very acidic conditions, the formation of valeric acid (VA) and γ-valerolactone (GVL) occur through surface-mediated and acid-catalyzed steps, while 4-hydroxyvaleric acid (HVA) is formed via an outer sphere electron transfer (OSET) route at higher pH (above the pKa of LA), with possible participation of a parallel electromediation path involving PbH_2. The pH-dependent charge states of the reactant molecule, coupled to possible collective effects of other evaluated parameters on double-layer structure, solvent dynamics, and side reactions (hydrogen evolution reaction, implantation, and hydride formation), led to a maximum faradaic efficiency for HVA production—amongst the tested conditions—being achieved at near-neutral pH, large negative potentials (staying above Pb cathodic corrosion limits), elevated temperature and reactant

concentration, and in the presence of K^+ ions. An HVA production rate higher than 40 g L^{-1} h^{-1} with >99.9 % selectivity, and conversion and faradaic efficiency both above 80% were shown. The rate is more than nine times higher than the highest recorded biochemical methods. Finally, an easy one-pot synthetic method to convert HVA into GVL with 100% selectivity and 96% conversion was also demonstrated.

Conflicts of interest

There are no conflicts to declare.

Acknowledgments

The authors acknowledge funding support from the National Science Foundation under CBET grant number 2004090.

References

1 J. E. Holladay, J. F. White, J. J. Bozell and D. Johnson, *Top value-added chemicals from biomass, Volume II - Results of Screening for Potential Candidates From Biorefinery Lignin*, 2007.

2 M. Signoretto, S. Taghavi, E. Ghedini and F. Menegazzo, *Molecules*, 2019, **24**, 2760.

3 S. I. Meramo Hurtado, P. Puello and A. Cabarcas, *ACS Omega*, 2021, **6**, 5627–5641.

4 S. Kang, J. Fu and G. Zhang, *Renewable and Sustainable Energy Reviews*, 2018, **94**, 340–362.

5 G. C. Hayes and C. R. Becer, *Polymer Chemistry*, 2020, **11**, 4068–4077.

6 F. D. Pileidis and M.-M. Titirici, *ChemSusChem*, 2016, **9**, 562–582.

7 Y. Du, X. Chen, J. Qi, P. Wang and C. Liang, *Catalysts*, 2020, **10**, 692.

8 H. Wu, J. Song, C. Xie, Y. Hu, P. Zhang, G. Yang and B. Han, *Chemical Science*, 2019, **10**, 1754–1759.

9 B. A. Frontana-Uribe, R. D. Little, J. G. Ibanez, A. Palma and R. Vasquez-Medrano, *Green Chemistry*, 2010, **12**, 2099.

10 O. Hammerich, B. Speiser and Editors., *Organic Electrochemistry: Revised and Expanded, Fifth Edition.*, CRC Press, Boca Raton, FL, 5th edn., 2016.

11 James Grimshaw, *Electrochemical Reactions and Mechanisms in Organic Chemistry*, Elsevier, Belfast, 2000, vol. 124.

12 G. G. Botte, *Interface magazine*, 2014, **23**, 49–55.

13 F. W. S. Lucas, R. G. Grim, S. A. Tacey, C. A. Downes, J. Hasse, A. M. Roman, C. A. Farberow, J. A. Schaidle and A. Holewinski, *ACS Energy Letters*, 2021, 1205–1270.

14 L. Xin, Z. Zhang, J. Qi, D. J. Chadderdon, Y. Qiu, K. M. Warsko and W. Li, *ChemSusChem*, 2013, **6**, 674–686.

15 T. R. dos Santos, P. Nilges, W. Sauter, F. Harnisch and U. Schröder, *RSC Advances*, 2015, **5**, 26634–26643.

16 Y. Qiu, L. Xin, D. J. Chadderdon, J. Qi, C. Liang and W. Li, *Green Chem.*, 2014, **16**, 1305–1315.

17 R. J. M. Bisselink, M. Crockatt, M. Zijlstra, I. J. Bakker, E. Goetheer, T. M. Slaghek and D. S. van Es, *ChemElectroChem*, 2019, **6**, 3285–3290.

18 P. Nilges, T. R. dos Santos, F. Harnisch and U. Schröder, *Energy Environ. Sci.*, 2012, **5**, 5231–5235.

19 Y. J. Yeon, H.-Y. Park and Y. J. Yoo, *Journal of Biotechnology*, 2015, **210**, 38–43.

20 C. Sathesh-Prabu and S. K. Lee, *Journal of Agricultural and Food Chemistry*, 2019, **67**, 2540–2546.

21 A. Steinbüchel, in *Biotechnology Set*, Wiley, 2001, pp. 403–464.

22 R. D. Ashby, D. K. Y. Solaiman, G. D. Strahan, C. Zhu, R. C. Tappel and C. T. Nomura, *Bioresource Technology*, 2012, **118**, 272–280.

23 P. Furrer, M. Zinn and S. Panke, in *Natural-Based Polymers for Biomedical Applications*, Elsevier, 2008, pp. 416–445.

24 G. Braunegg, G. Lefebvre and K. F. Genser, *Journal of Biotechnology*, 1998, **65**, 127–161.

25 Research and Markets, Global Bioplastics & Biopolymers Market Outlook 2020-2025, https://www.globenewswire.com/news-release/2020/04/17/2017839/0/en/Global-Bioplastics-Biopolymers-Market-Outlook-2020-2025.html, (accessed April 22, 2021).

26 N. Goonoo, A. Bhaw-Luximon, P. Passanha, S. R. Esteves and D. Jhurry, *Journal of Biomedical Materials Research Part B: Applied Biomaterials*, 2017, **105**, 1667–1684.

27 E. Gabirondo, A. Sangroniz, A. Etxeberria, S. Torres-Giner and H. Sardon, *Polymer Chemistry*, , DOI:10.1039/D0PY00088D.

28 R. Ganesh Saratale, S.-K. Cho, G. Dattatraya Saratale, A. A. Kadam, G. S. Ghodake, M. Kumar, R. Naresh Bharagava, G. Kumar, D. Su Kim, S. I. Mulla and H. Seung Shin, *Bioresource Technology*, 2021, 124685.

29 D. Kim, C. Sathesh-Prabu, Y. JooYeon and S. K. Lee, *Journal of Agricultural and Food Chemistry*, 2019, **67**, 10678–10684.

30 Y. J. Yeon, H.-Y. Park and Y. J. Yoo, *Bioresource Technology*, 2013, **134**, 377–380.

31 H. Miyake, S. Ye and M. Osawa, *Electrochemistry Communications*, 2002, **4**, 973–977.

32 F. W. S. Lucas and F. H. B. Lima, *ChemElectroChem*, 2020, **7**, 3733–3742.

33 C. J. Bondue and M. T. M. Koper, *Journal of Catalysis*, 2019, **369**, 302–311.

34 E. L. Martin, in *Organic Reactions*, John Wiley & Sons, Inc., Hoboken, NJ, USA, 2011, pp. 155–209.

35 S. D. Argade and E. Gileadi, in *Electrosorption*, Springer US, Boston, MA, 1967, pp. 87–115.

36 D. Strmcnik, M. Uchimura, C. Wang, R. Subbaraman, N. Danilovic, D. van der Vliet, A. P. Paulikas, V. R. Stamenkovic and N. M. Markovic, *Nature Chemistry*, 2013, **5**, 300–306.

37 X. Wang, C. Xu, M. Jaroniec, Y. Zheng and S.-Z. Qiao, *Nature Communications*, 2019, **10**, 4876.

38 B. N. Kabanov, I. I. Astakhov and I. G. Kiseleva, *Russian Chemical Reviews*, 1965, **34**, 775–785.

39 H. W. Salzberg, *Journal of The Electrochemical Society*, 1953, **100**, 146.

40 L. W. Gastwirt and H. W. Salzberg, *Journal of The Electrochemical Society*, 1957, **104**, 701.

41 A. Frumkin, V. Korshunov and I. Bagozkaya, *Electrochimica Acta*, 1970, **15**, 289–301.

42 M. Pourbaix, *Atlas of Electrochemical Equilibria in - Aqueous Solutions*, National Association of Corrosion Engineers & International Cebelcor, Houston, Texas, Second Eng., 1974.

43 I. Ledezma-Yanez, W. D. Z. Wallace, P. Sebastián-Pascual, V. Climent, J. M. Feliu and M. T. M. Koper, *Nature Energy*, 2017, **2**, 17031.

44 D. C. Grahame, *Journal of The Electrochemical Society*, 1951, **98**, 343.

45 B. Huang, K. H. Myint, Y. Wang, Y. Zhang, R. R. Rao, J. Sun, S. Muy, Y. Katayama, J. Corchado Garcia, D. Fraggedakis, J. C. Grossman, M. Z. Bazant, K. Xu, A. P. Willard and Y. Shao-Horn, *The Journal of Physical Chemistry C*, 2021, acs.jpcc.0c10492.

46 N. Danilovic, R. Subbaraman, D. Strmcnik, A. P. Paulikas, D. Myers, V. R. Stamenkovic and N. M. Markovic, *Electrocatalysis*, 2012, **3**, 221–229.

47 D. R. Lide, W. M. M. Haynes, G. Baysinger, L. I. Berger, D. L. Roth, D. Zwillinger, M. Frenkel and R. N. Goldberg, *Journal of the American Chemical Society*, 2009, **131**, 12862–12862.

48 P. Koley, B. S. Rao, S. C. Shit, Y. Sabri, J. Mondal, J. Tardio and N. Lingaiah, *Fuel*, 2021, **289**, 119900.

49 Y. Xu, H. Zhang, H. Li and S. Yang, *Current Green Chemistry*, 2020, **7**, 304–313.

50 R. Xu, K. Liu, H. Du, H. Liu, X. Cao, X. Zhao, G. Qu, X. Li, B. Li and C. Si, *ChemSusChem*, 2020, **13**, 6461–6476.